



CRACK SIZE IDENTIFICATION USING AN EXPANDED MODE METHOD

T. Y. KAM and T. Y. LEE

Department of Mechanical Engineering, National Chiao Tung University, Hsin Chu 30050, Taiwan, Republic of China

(Received 21 April 1993; in revised form 15 October 1993)

Abstract—An expanded mode method constructed based on the modal analysis method and an energy approach is presented for size identification of a crack with given location in a damaged structure. Measured natural frequencies and mode shapes of the structure with or without a crack are used to compute the strain energies of the structures subject to free vibration via a quasi-static approach. The two types of strain energy are then combined with the work required for the crack formation to construct the energy balance equation from which the size of the crack is evaluated through an iteration procedure. The theory of fracture mechanics is used to derive the work required for crack formation. Examples of the identification of crack sizes for a number of damaged beam structures are given to illustrate the applications of the proposed expanded mode method. Factors affecting the accuracy of crack size identification are investigated using a cracked cantilever beam as an example. The results show that the present method is promising for practical applications.

1. INTRODUCTION

Vibration investigation of damaged structures has been proved to be a feasible approach for fault diagnosis. Utilizing the fact that a crack introduces a local flexibility which can change the dynamic behavior of the structure, many researchers have proposed methods for the identification of crack location and/or crack size from measured vibration frequencies and mode shapes of cracked structures (e.g. Cawley and Adams, 1979; Anifantis *et al.*, 1983; Inagaki *et al.*, 1981; Rizos and Aspragathos, 1990; Shen, 1989; Chondros and Dimarogonas, 1980). Recently, the authors (Kam and Lee, 1992; Lee and Kam, 1993) have developed methods for crack detection using measured vibration data of damaged structures via an energy approach. It was found that the proposed energy approach for crack detection is promising to become an effective nondestructive evaluation method and hence deserves further study.

In this paper, an expanded mode method evolved from the modal analysis method and fracture mechanics principles is developed for size identification of a crack in damaged structures using measured vibration data. In the present analysis, it is assumed that the evaluation of crack location can be achieved by using the method proposed by Lee and Kam (1993). Based on the previously proposed energy approach (Kam and Lee, 1992), strain energies of a structure with or without a crack subject to free vibration and the work for the crack formation are used to construct the energy balance equation from which the crack size is determined via an iteration procedure. Herein the strain energies of the uncracked and cracked structures induced by free vibration are evaluated by utilizing measured frequencies and mode shapes of the structures via the proposed expanded mode method. The work required for the crack formation is determined using an expression derived from the theory of fracture mechanics. In the present method, except measured frequencies and mode shapes of the structure with or without a crack and the basic material properties of the structure, no other information (including the stiffness matrices of the uncracked and cracked structures) is needed in the identification process. The feasibility and applications of the proposed method are demonstrated by means of several examples of the identification of sizes of cracks located at different positions in beams and frames. Factors affecting the accuracy of crack size identification are investigated using a cracked cantilever beam as an example.

2. ENERGY BALANCE EQUATION

According to the Griffith balance of energy, a crack can form in an elastic body only if such a process causes the total potential energy of the body to decrease. The total potential energy, π , of a loaded body is defined as

$$\pi = U - F, \tag{1}$$

where U is strain energy and F the work done by external forces. An incremental increase in the crack area, dA , under equilibrium conditions can be expressed as (Anderson, 1991)

$$-\frac{d\pi}{dA} = \frac{dW_c}{dA}, \tag{2}$$

where W_c is the work required to create a new crack surface.

The energy balance equation for the case where the crack size grows from zero to a is obtained by integrating both sides of eqn (2):

$$-\pi(a) + \pi(0) = W_c(a) - W_c(0). \tag{3}$$

Since no work is required for creating a crack with zero size, the above equation becomes

$$-\pi(a) + \pi(0) = W_c(a). \tag{4}$$

Next consider the case in which the body is subjected to a dead load, as shown in Fig. 1a. The work done by the applied load and the strain energy stored in the body are, respectively,

$$F = P \cdot \delta \tag{5}$$

and

$$U = \frac{P\delta}{2} = \frac{F}{2}. \tag{6}$$

Substitution of the above two equations into eqn (1) yields

$$\pi = -U. \tag{7}$$

Therefore, the energy balance equation of eqn (4) can be written as

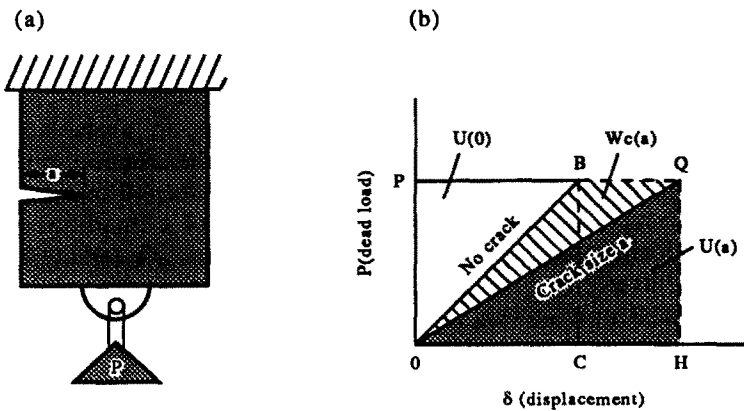


Fig. 1. Energies of an elastic body with or without a crack subject to dead load.

$$U(a) - U(0) = W_c(a) \quad (8a)$$

or

$$U(a) = U(0) + W_c(a). \quad (8b)$$

The above relation is demonstrated graphically in Fig. 1b. The strain energy of the body without a crack, $U(0)$, is denoted by the area of the triangle $\triangle OBP$; the work done for creating crack size a , $W_c(a)$, is represented by the shaded area of $\triangle OQB$; the strain energy of the body with a crack of crack size a , $W(a)$, is the area of $\triangle OHQ$. Apparently $U(a)$ is the sum of $U(0)$ and $W_c(a)$.

3. EXPANDED MODE METHOD

Consider the free vibration of a damaged structure containing a crack of size a , which has been modeled as an MDOF system. If the mode shapes and the corresponding vibration frequencies obtained from modal tests are, respectively, ϕ_i and $\lambda_i = (\omega_i^2)$, $i = 1, 2, \dots, N$, the response of the MDOF system can be expressed as

$$\mathbf{V} = \Phi \mathbf{Y}, \quad (9)$$

where \mathbf{V} is the $N \times 1$ displacement vector, Φ is the $N \times N$ mode shape matrix, which is a collection of ϕ_i , and \mathbf{Y} is the $N \times 1$ vector of generalized coordinates. The mode shape matrix has the following orthogonality properties:

$$\lambda = \Phi^T \mathbf{K} \Phi \quad (10)$$

and

$$\mathbf{I} = \Phi^T \mathbf{M} \Phi, \quad (11)$$

where λ is the diagonal matrix of square values of frequencies (ω_i^2), \mathbf{M} is the mass matrix, \mathbf{I} is the identity matrix, \mathbf{K} is the system stiffness matrix and the superscript T denotes the transpose of a matrix. The strain energy, $U(a)$, stored in the cracked structure during vibration is obtained as

$$U(a) = \frac{1}{2} \mathbf{V}^T \mathbf{K} \mathbf{V}. \quad (12)$$

In view of eqns (9) and (10), the strain energy in eqn (12) can be expressed as the sum of the modal strain energies of the system, i.e.

$$U(a) = \frac{1}{2} \mathbf{Y}^T \lambda \mathbf{Y} = \frac{1}{2} \sum_{i=1}^N Y_i \lambda_i Y_i. \quad (13)$$

Consider a cracked structure vibrating at the shape of mode i . The response of mode i subject to free vibration with nonzero initial velocity $\dot{Y}_i(0)$ is (Clough and Penzien, 1975)

$$Y_i(t) = \frac{\dot{Y}_i(0)}{\omega_i} \sin \omega_i t. \quad (14)$$

In view of eqns (13) and (14), it can be shown that the maximum modal strain energy of mode i is

$$\hat{U}_i(a) = \frac{1}{2} \dot{Y}_i^2(0), \quad (15)$$

where $\hat{U}_i(a)$ is the maximum modal strain energy of mode i . Again, in view of eqns (9) and

(14), the maximum modal inertia force of mode i can be written as (Clough and Penzien, 1975)

$$\mathbf{f}_i = \mathbf{M}(\ddot{\mathbf{V}}_i)_{\max} = \mathbf{M}\boldsymbol{\phi}_i\omega_i\dot{Y}_i(0), \quad (16)$$

where $(\ddot{\mathbf{V}}_i)_{\max}$ is the maximum acceleration. It is noted that the maximum modal strain energy of eqn (15) is also equal to the strain energy of the structure loaded statically by the inertia force of eqn (16).

Next, consider the evaluation of the strain energy of the same structure but without a crack loaded statically by the inertia force of eqn (16). Assuming that the stiffness matrix of the uncracked structure is unavailable, then the strain energy of the structure cannot be determined directly from a finite element analysis. Herein a quasi-static expanded mode method constructed based on simple vibration theory is introduced for evaluating the strain energy of a free vibrating uncracked structure at the time when the inertia force of the uncracked structure closely approximates that of eqn (16). In view of eqn (16), the inertia force of the uncracked structure subject to free vibration at any instant is expressed as

$$\tilde{\mathbf{f}}_i(t) = \mathbf{M}\ddot{\tilde{\mathbf{V}}}(t) = \mathbf{M}\tilde{\boldsymbol{\Phi}}\tilde{\boldsymbol{\lambda}}\tilde{\mathbf{Y}}(t), \quad (17)$$

where $\tilde{\mathbf{f}}_i$, $\ddot{\tilde{\mathbf{V}}}$, $\tilde{\boldsymbol{\Phi}}$, $\tilde{\boldsymbol{\lambda}}$ and $\tilde{\mathbf{Y}}$ are the nodal inertia force vector, nodal acceleration vector, mode shape matrix, natural frequency matrix and the vector of generalized coordinates of the uncracked structure, respectively; t denotes time. It is assumed that the existence of a crack does not affect the mass of the structure. Hence, the mass matrices of the cracked and uncracked structures are the same. Imagine that at some specific time, say $t = \tilde{t}$, the inertia force of the uncracked structure closely approximates the value of the inertia force in eqn (16), i.e.

$$\mathbf{f}_i \cong \tilde{\mathbf{f}}_i(\tilde{t}) = \mathbf{M}\tilde{\boldsymbol{\phi}}\tilde{\boldsymbol{\lambda}}\tilde{\mathbf{Y}}(\tilde{t}). \quad (18)$$

The above approximation equation implies that the synthesis of several modal inertia forces of the uncracked structure may yield the approximate or hopefully the exact value of the i th maximum modal inertia force of the cracked structure at some specific time. Therefore, the solution of eqn (18) gives the (approximate) deflection of the uncracked structure loaded statically by the modal inertia force of eqn (16). The premultiplication of eqn (18) by $\tilde{\boldsymbol{\Phi}}^T$ leads to

$$\tilde{\boldsymbol{\Phi}}^T\mathbf{f}_i = \tilde{\boldsymbol{\Phi}}^T\mathbf{M}\tilde{\boldsymbol{\Phi}}\tilde{\boldsymbol{\lambda}}\tilde{\mathbf{Y}}(\tilde{t}). \quad (19)$$

Observing the orthogonality condition of the mode shape matrix with respect to the mass matrix, eqn (19) can be rewritten as

$$\tilde{\boldsymbol{\Phi}}^T\mathbf{f}_i = \tilde{\boldsymbol{\lambda}}\tilde{\mathbf{Y}}(\tilde{t}). \quad (20)$$

Premultiplying the above equation by the inverse of $\tilde{\boldsymbol{\lambda}}$, $\tilde{\boldsymbol{\lambda}}^{-1}$, one gets an expression for evaluating $\tilde{\mathbf{Y}}$:

$$\tilde{\mathbf{Y}}(\tilde{t}) = \tilde{\boldsymbol{\lambda}}^{-1}\tilde{\boldsymbol{\Phi}}^T\mathbf{f}_i. \quad (21)$$

It is noted that the time \tilde{t} is a dummy in the above equation and the accuracy of $\tilde{\mathbf{Y}}(\tilde{t})$ can be improved by increasing the number of modes of the uncracked structure, i.e. the sizes of $\tilde{\boldsymbol{\lambda}}$ and $\tilde{\boldsymbol{\Phi}}$, in the above equation. In view of eqn (13), the approximate strain energy of the uncracked structure, $U(0)$, subject to the modal inertia force of the cracked structure can then be written as

$$U(0) = \frac{1}{2} \tilde{\mathbf{Y}}^T \tilde{\lambda} \tilde{\mathbf{Y}}. \quad (22)$$

It is worth mentioning here that, although the above strain energy is derived from the synthesis of several vibration modes of the uncracked structure, as will be shown by the results obtained from the following numerical investigation, even the use of only one vibration mode can yield a very good approximation of the exact strain energy of the uncracked structure subject to the modal inertia force of eqn (16). Assuming that the strain energy of the uncracked structure obtained from eqn (22) is "exact" when loaded by the modal inertia force of the cracked structure, the discrepancy between eqns (15) and (22) is equal to the work required for crack formation, as described in the previous section. If no crack exists in the structure, both eqns (15) and (22) will yield the same result. It is also worth noting that only the translation degrees of freedom are needed in constructing the mode shape matrices of the cracked and uncracked structures in eqns (16) and (21), in which the effects of rotational degrees of freedom can be included via the use of the static condensation method.

4. DETERMINATION OF CRACK SIZE

The work required for crack formation, W_c , has been studied extensively in fracture mechanics and expressions for evaluating the work for different problems are available in the literature (Broek, 1974). Consider a crack in a beam-type structure; the work for crack formation is expressed as (Tada *et al.*, 1973)

$$W_c = b \int_0^a [(K_I^2 + K_{II}^2)/E' + (1 + \nu)K_{III}^2/E] da, \quad (23)$$

where a is crack length, b is width of beam section, $E' = E$ for plane stress, $E' = E/(1 - \nu^2)$ for plane strain, E is the elastic modulus, ν is the Poisson ratio, and K_I , K_{II} and K_{III} are stress intensity factors for opening type, sliding type and tearing type cracks, respectively. Now consider the work required for creating a crack of size a in a beam structure subject to the i th maximum modal inertia force. With the action of axial force neglected, eqn (23) becomes

$$W_c = b \int_0^a \{[(K_{IM} + K_{IP})^2 + K_{IIP}^2]/E'\} da, \quad (24)$$

where

$$K_{IM} = \left(\frac{6M}{bh^2}\right) \sqrt{\pi a} F_1(s) \quad (25)$$

$$K_{IP} = \left(\frac{3Pl}{bh^2}\right) \sqrt{\pi a} F_1(s) \quad (26)$$

$$K_{IIP} = \left(\frac{P}{bh}\right) \sqrt{\pi a} F_{II}(s) \quad (27)$$

$$F_1(s) = \sqrt{\left(\frac{2}{\pi s}\right) \tan\left(\frac{\pi s}{2}\right)} \frac{0.923 + 0.199 \left[1 - \sin\left(\frac{\pi s}{2}\right)\right]^4}{\cos\left(\frac{\pi s}{2}\right)} \quad (28)$$

$$F_{II}(s) = (3s - 2s^2) \frac{1.122 - 0.561s + 0.085s^2 + 0.18s^3}{\sqrt{1-s}}, \tag{29}$$

with $s = a/h$; b and h are the width and depth of beam cross-section, respectively, l is the distance between the crack and the right end of the cracked member, and M and P are the moment and shear force, respectively, at the right end of the cracked member. As mentioned before, the maximum modal strain energy of the cracked beam structure can be expressed as the sum of the strain energy of the uncracked beam structure subject to the maximum modal inertia force of the cracked beam structure and the work required for the crack formation. In view of eqns (15), (22) and (24), the energy balance equation for the beam structure can be established as

$$\hat{U}_i(a) = U(0) + W_c. \tag{30}$$

In the above equation, both $\hat{U}_i(a)$ and $U(0)$ can be evaluated immediately once the mode shapes and vibration frequencies of the cracked and uncracked beam structures have been measured by experiment and the value of $\dot{Y}_i(0)$ in eqn (15) is chosen. The magnitude of the crack can then be determined from eqn (30) using a Newton-Raphson type iteration scheme. The value of $\dot{Y}_i(0)$ can be chosen arbitrarily and it has no effect on the identified crack size.

5. SENSITIVITY ANALYSIS

The existence of noise in measured vibration data is inevitable. Therefore, the measured vibration frequencies and mode shapes may deviate from the true values of the uncracked as well as the cracked structures. An approximate analysis in the field of probability (Benjamin and Cornell, 1970) is used to investigate how the variations in vibration frequencies and mode shapes affect the accuracy of the identified crack size. Herein, vibration frequencies, mode shapes and crack size are treated as random variables. Let (\bar{X}, σ_x) be the expected value and standard deviation pair of random variable X . In view of eqn (30), we define the function $G(\mathbf{X})$ as

$$G(\mathbf{X}) = \hat{U}_i(a) - U(0) - W_c(a) = 0, \tag{31}$$

where $\mathbf{X} = \{\omega_i, \phi_{i1}, \dots, \phi_{im}, \tilde{\omega}_1, \dots, \tilde{\omega}_p, \tilde{\phi}_{11}, \dots, \tilde{\phi}_{pq}, a\}$. We expand $G(\mathbf{X})$ at the mean values of all random variables in a truncated Taylor series:

$$G(\mathbf{X}) \doteq G(\bar{\mathbf{X}}) + (\omega_i - \bar{\omega}_i) \left. \frac{\partial G}{\partial \omega_i} \right|_{\bar{\mathbf{X}}} + \sum_{j=1}^m (\phi_{ij} - \bar{\phi}_{ij}) \left. \frac{\partial G}{\partial \phi_{ij}} \right|_{\bar{\mathbf{X}}} + \sum_{l=1}^p (\tilde{\omega}_l - \bar{\tilde{\omega}}_l) \left. \frac{\partial G}{\partial \tilde{\omega}_l} \right|_{\bar{\mathbf{X}}} + \sum_{j=1}^p \sum_{k=1}^q (\tilde{\phi}_{jk} - \bar{\tilde{\phi}}_{jk}) \left. \frac{\partial G}{\partial \tilde{\phi}_{jk}} \right|_{\bar{\mathbf{X}}} + (a - \bar{a}) \left. \frac{\partial G}{\partial a} \right|_{\bar{\mathbf{X}}}, \tag{32}$$

where p is number of frequencies, m and q are numbers of degrees of freedom, and $\bar{\mathbf{X}}$ stands for the expected values of all random variables.

The first-order approximation to the expected value of G is

$$E[G] \doteq G(\bar{\mathbf{X}}) = \hat{U}_i(\bar{a}) - \bar{U}(0) - \bar{W}_c(\bar{a}) = 0. \tag{33}$$

The first-order approximation to the variance of G is

$$\begin{aligned} \text{Var}[G] \doteq & \left(\frac{\partial G}{\partial \omega_i} \bigg|_{\mathbf{x}} \right)^2 \text{Var}[\omega_i] + \sum_{j=1}^m \left(\frac{\partial G}{\partial \phi_{ij}} \bigg|_{\mathbf{x}} \right)^2 \text{Var}[\phi_{ij}] + \sum_{l=1}^p \left(\frac{\partial G}{\partial \tilde{\omega}_l} \bigg|_{\mathbf{x}} \right)^2 \\ & + \text{Var}[\tilde{\omega}_l] + \sum_{l=1}^p \sum_{k=1}^q \left(\frac{\partial G}{\partial \tilde{\phi}_{lk}} \bigg|_{\mathbf{x}} \right)^2 \text{Var}[\tilde{\phi}_{lk}] + \left(\frac{\partial G}{\partial a} \bigg|_{\mathbf{x}} \right)^2 \text{Var}[a] = 0, \quad (34) \end{aligned}$$

where $\text{Var}[X] = \sigma_x^2$, the variance of X .

The expected value of crack size a is evaluated from eqn (33) following the iteration procedure described in the previous section. The variance of crack size can be easily obtained from eqn (34), i.e.

$$\begin{aligned} \text{Var}[a] = & \frac{-1}{\left(\frac{\partial G}{\partial a} \bigg|_{\mathbf{x}} \right)^2} \left\{ \left(\frac{\partial G}{\partial \omega_i} \bigg|_{\mathbf{x}} \right)^2 \text{Var}[\omega_i] + \sum_{j=1}^m \left(\frac{\partial G}{\partial \phi_{ij}} \bigg|_{\mathbf{x}} \right)^2 \right. \\ & \times \text{Var}[\phi_{ij}] + \sum_{l=1}^p \left(\frac{\partial G}{\partial \tilde{\omega}_l} \bigg|_{\mathbf{x}} \right)^2 \text{Var}[\tilde{\omega}_l] + \sum_{l=1}^p \sum_{k=1}^q \left(\frac{\partial G}{\partial \tilde{\phi}_{lk}} \bigg|_{\mathbf{x}} \right)^2 \text{Var}[\tilde{\phi}_{lk}] \left. \right\}. \quad (35) \end{aligned}$$

6. EXAMPLES

The aforementioned method for crack size evaluation will be applied to the determination of the magnitudes of cracks on several beam structures. First, consider a 300 mm cracked cantilever beam of cross-section $20 \times 20 \text{ mm}^2$, with modulus of elasticity $E = 2.06 \times 10^5 \text{ MPa}$, Poisson's ratio $\nu = 0.3$ and mass density $\rho = 7750 \text{ kg/m}^3$ (Fig. 2a). Herein the measured vibration frequencies and mode shapes of the beam containing an edge crack of various sizes at different positions along the beam were obtained by using a finite element analysis of the cracked beam (see Fig. 2b). The cracked element developed by Qian *et al.* (1990), which has been validated by experimental data, was used in the above finite element analysis. Some typical natural frequencies of the first three modes of the cracked beam containing a crack of various sizes and locations are given in Table 1. Once the vibration characteristics of the uncracked and cracked beams are known, the sizes of the crack with given locations can be estimated using any set of eigencouples (frequency and mode shape) of the first three modes of the cracked beam. In the identification process, however, the number of vibration modes used in evaluating the strain energy of the uncracked beam of eqn (22) may affect the accuracy of the strain energy, depending on

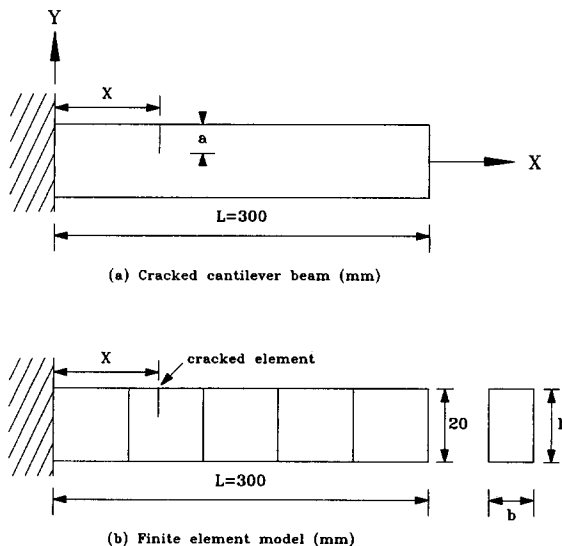


Fig. 2. Cracked cantilever beam and its finite element model for crack detection.

Table 1. Natural frequencies of cracked cantilever beams

Crack (mm)		Natural frequency (Hz)		
Position	Depth	1st	2nd	3rd
30	2	183.09	1155.85	3256.39
	6	167.24	1122.64	3235.00
	10	136.53	1072.96	3202.93
	14	93.39	1026.86	3169.97
90	2	184.14	1158.99	3243.39
	6	176.02	1146.47	3120.12
	10	156.78	1119.47	2904.84
	14	120.08	1078.18	2666.37
150	2	184.77	1152.49	3259.41
	6	181.91	1087.76	3258.83
	10	173.93	956.79	3256.18
	14	152.58	771.14	3249.13
210	2	185.04	1155.97	3236.75
	6	184.54	1116.07	3061.41
	10	183.07	1014.00	2753.37
	14	178.18	802.39	2421.45
270	2	185.09	1160.29	3256.36
	6	185.08	1158.29	3227.39
	10	185.04	1152.18	3138.28
	14	184.92	1130.86	2844.58
No crack		185.20	1160.60	3259.10

which mode of the cracked beam is chosen. To demonstrate the accuracy of the present method, different synthesis methods were adopted in the following illustration. Only the eigencouple of the first mode of the uncracked beam would be used if the eigencouple of the first mode of the cracked beam was chosen for identification; if the second mode of the cracked beam was adopted, the first two modes of the uncracked beam would be used; the first three modes of the uncracked beam would be used if the third mode of the cracked beam was chosen (this policy was also adopted for the other structures considered in the other examples). The maximum modal strain energies of the cracked beam and the corresponding strain energies of the uncracked beam for different cases were first computed by using, respectively, eqns (15) and (22), and the values are listed in Table 2. Based on eqn (30), the sizes of the crack at different locations were determined via a Newton-Raphson type iteration scheme. The identified crack sizes and the corresponding errors in estimation are given in Table 3. Figures 3-5 illustrate the discrepancies between the actual and identified crack sizes. The results show that the overall performance of the present method is excellent for the cases considered, except for cracks of small sizes located at any node of the chosen vibrating mode of the cracked beams. For instance, a crack of any size located at 150 mm can be identified accurately using either the first or the second modes; for the same crack, even though it is located at the first node ($x = 150$ mm) of the third mode, the use of the third mode of the cracked beam can still yield good results for crack sizes larger than 2 mm (see Table 3). It is also worth noting that, since there is no node in the first vibration mode of the cantilever beam, the use of the first modes of both the cracked and uncracked beams in the identification process can yield excellent results. In the above identification process, several factors may have some adverse affects on the accuracy of the identified crack size. One of these factors is number of elements. The effect of number of elements on the accuracy of the identified crack size was first studied. The identified crack sizes for the cracked beam discretized into, respectively, two, three and four elements are listed in Table 4 in comparison with the exact crack sizes. It is noted that the effects of number of elements are minimal and this reaffirms the effectiveness of the present identification method. The next factor to be considered is the uncertainties existing in measurement. Variations in measured eigencouples are inevitable and their effects on the accuracy of identified crack size must be investigated. The aforementioned approximate analysis [see eqns (33) and (35)] was used to study the variations in identified crack size induced by those

Table 2. Strain energies of cantilever beams with and without a crack†

Crack		1st mode		2nd mode		3rd mode	
Position (mm)	Depth (mm)	$\hat{U}_1(a)$	$U(0)$	$\hat{U}_2(a)$	$U(0)$	$\hat{U}_3(a)$	$U(0)$
30	2	1404.830	1374.580	857.359	850.638	487.026	486.129
	6	1373.330	1120.890	879.447	833.453	495.778	490.112
	10	1320.260	716.880	918.821	846.503	507.980	499.383
	14	1263.960	320.040	962.474	908.260	517.886	509.258
90	2	1410.100	1395.650	850.490	848.291	486.798	482.058
	6	1419.050	1283.270	817.036	799.016	497.195	460.140
	10	1437.730	1030.780	745.247	706.528	527.948	454.373
	14	1464.920	614.533	637.360	596.979	586.829	515.453
150	2	1411.350	1406.490	850.516	838.847	485.336	485.344
	6	1432.050	1383.014	816.405	720.464	482.163	481.975
	10	1486.950	1311.020	735.514	527.235	475.858	474.947
	14	1614.530	1084.950	574.803	359.331	467.389	464.586
210	2	1410.080	1409.270	859.888	853.170	482.457	475.799
	6	1419.890	1411.500	904.302	835.304	449.260	400.475
	10	1449.050	1417.270	994.129	751.861	356.589	281.918
	14	1543.590	1427.000	1066.680	518.981	207.087	170.006
270	2	1409.070	1409.050	855.270	854.950	487.215	486.277
	6	1409.570	1409.360	862.106	858.798	500.137	490.067
	10	1411.080	1410.320	882.844	869.941	534.535	492.013
	14	1416.230	1413.550	953.121	901.495	588.744	423.575

† $\hat{U}_i(a)$: strain energy of cracked structure vibrating at mode i ; $U_i(0)$: strain energy of uncracked structure. The units of strain energy are $\text{kg}-\text{m}^2/\text{s}^2$.

in measured eigencouples. Figure 6 shows the coefficient of variation (cov) of a crack with different sizes in element 1 subject to various degrees of uncertainties in measured eigencouples. It is noted that the variation in crack size can be less than 5% if the variations in measured frequencies and mode shapes are either less than 5% or the size of the crack is relatively large (>6 mm for the cases considered). From actual tests for crack size

Table 3. Actual and identified crack sizes of cantilever beams

Actual (target) crack		1st mode		Identified crack size 2nd mode		3rd mode	
Position (mm)	Depth (mm)	Depth (mm)	Error %	Depth (mm)	Error %	Depth (mm)	Error %
30	2	2.0097	0.4850	2.0123	0.6150	2.0367	1.8350
	6	6.0027	0.0450	6.0044	0.0733	6.0128	0.2133
	10	10.0011	0.0110	10.0355	0.3550	10.0108	0.1080
	14	14.0004	0.0029	14.0153	0.1093	14.0139	0.0993
90	2	2.0100	0.5000	2.0142	0.7100	2.0100	0.5000
	6	6.0030	0.0500	6.0091	0.1517	6.0103	0.1717
	10	10.0010	0.0100	10.0242	0.2420	10.0265	0.2650
	14	14.0003	0.0021	14.0557	0.3979	14.0494	0.3529
150	2	2.0100	0.5000	2.0098	0.4900	2.8815	44.0750
	6	6.0065	0.1083	6.0054	0.0900	6.1382	2.3033
	10	10.0018	0.0180	10.0015	0.0150	10.0531	0.5310
	14	14.0017	0.0121	14.0023	0.0164	14.0338	0.2414
210	2	2.0000	0.0000	2.0105	0.5250	2.0102	0.5100
	6	6.0030	0.0500	6.0093	0.1550	6.0113	0.1883
	10	10.0021	0.0210	10.0216	0.2160	10.0270	0.2700
	14	14.0019	0.0136	14.0222	0.1586	14.0399	0.2850
270	2	2.0140	0.7000	2.0156	0.7800	2.0156	0.7800
	6	6.0800	1.3333	6.0047	0.0783	6.0192	0.3200
	10	9.9900	0.1000	10.0072	0.0720	10.0638	0.6380
	14	14.0030	0.0214	14.0673	0.4807	14.1119	0.7993

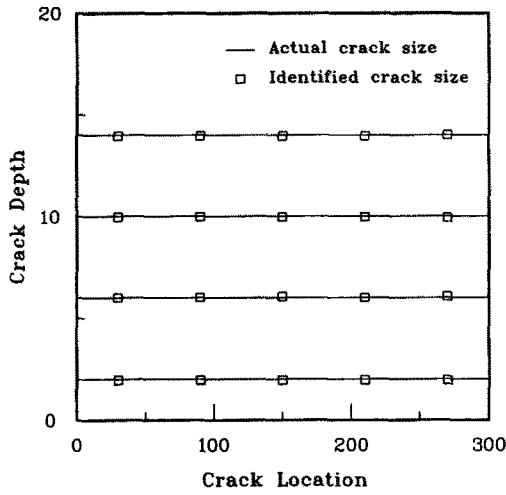


Fig. 3. Crack size identification of a cantilever beam using the first mode (mm).

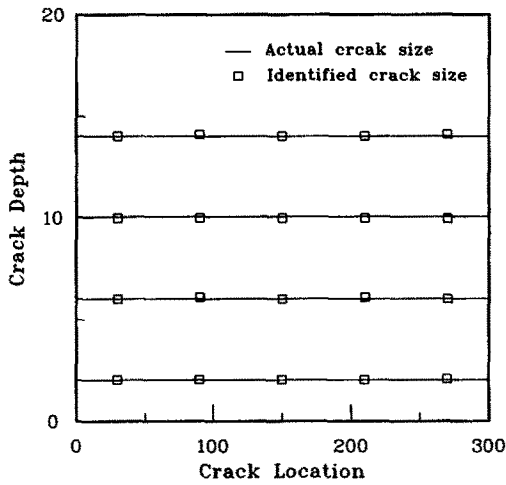


Fig. 4. Crack size identification of a cantilever beam using the second mode (mm).

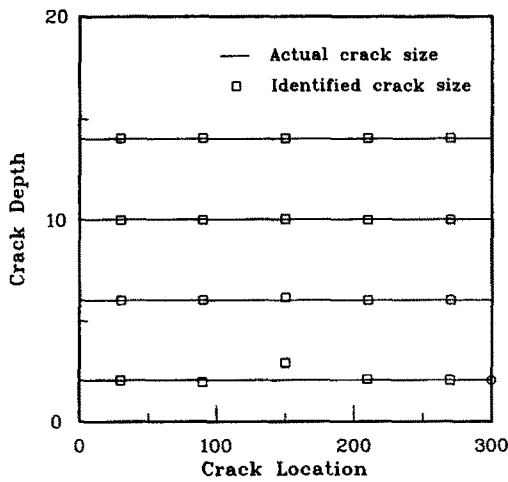


Fig. 5. Crack size identification of a cantilever beam using the third mode (mm).

Table 4. Actual and identified crack sizes using different finite element models of cantilever beams

Finite element model	Actual (target) crack		Identified crack size		
	No. of elements	Position (mm)	Depth (mm)	Error %	
2	75.0	2	2.0263	1.3150	
			6	6.0068	0.1133
		225.0	10	10.0040	0.0400
			14	13.9780	0.1571
			2	2.0400	2.0000
			6	6.0108	0.1800
	3	50.0	10	10.0016	0.0160
			14	14.0004	0.0029
			2	2.0167	0.8350
			6	6.0044	0.0733
		250.0	10	10.0028	0.0280
			14	14.0011	0.0079
2	2.0285		1.4250		
6	6.0074		0.1233		
4	187.5	10	10.0021	0.0210	
		14	14.0001	0.0007	
		2	2.0030	0.1500	
		6	6.0036	0.0600	
		262.5	10	10.0024	0.0240
			14	14.0006	0.0043
	2		2.0264	1.3200	
	6		6.0071	0.1183	

identification (Lee, 1992), it was found that uncertainties in measurement can be greatly reduced if the tests are performed carefully.

The last factor to be considered is location of the crack in the cracked element. It is noted that a crack is likely to develop near the critical part of the beam. Herein a crack at various positions in element 2 is used as an example to illustrate the effects of crack location on the accuracy of identified crack size. Figure 7 shows the errors of identified crack sizes for a crack of different sizes at various positions in element 2. It is noted that the error increases as the crack approaches either one of the boundaries of the cracked element. The

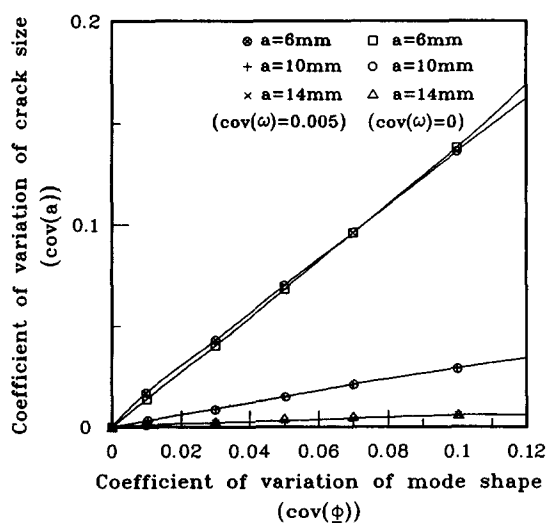


Fig. 6. Variation of crack size induced by variations of measured eigencouple.

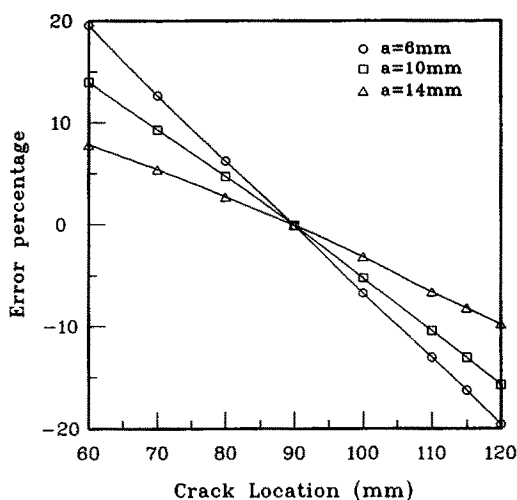


Fig. 7. Errors of identified crack sizes for cracks located at various positions in the second element.

increase in the number of elements or remeshing elements with different sizes for the evaluation of strain energies may help to improve the accuracy of identified crack size. It is therefore advised that different finite element meshes be used in the identification process to check the convergence of the identified crack size. It is also worth mentioning here that although the identification of crack location has not been discussed in this paper, the approximate location of a crack in a structure can be easily determined by the identification of the cracked element (Lee and Kam, 1993).

The identification of cracks of various sizes located at different positions along a free-free beam was performed. The material properties and dimensions of the fixed end beam were adopted for this example. The natural frequencies of the first three modes of the beam containing cracks of various sizes and located at different positions are given in Table 5. Using the present method, the sizes of the cracks located at different positions were identified. The maximum modal strain energies of the cracked beam and the corresponding

Table 5. Natural frequencies of cracked free-free beam

Crack (mm)		Natural frequency (Hz)		
Position	Depth	1st	2nd	3rd
30	2	1178.10	3253.77	6411.65
	6	1175.97	3224.94	6282.52
	10	1169.45	3136.30	5924.96
	14	1146.68	2844.24	5165.55
90	2	1173.30	3234.44	6413.86
	6	1128.98	3061.72	6328.67
	10	1015.39	2759.87	6201.36
	14	778.55	2438.29	6080.38
150	2	1168.08	3256.83	6395.72
	6	1084.58	3256.38	6173.54
	10	910.79	3253.92	5819.16
	14	642.64	3246.86	5468.32
210	2	1173.30	3234.44	6413.86
	6	1128.98	3061.72	6328.67
	10	1015.39	2759.87	6201.36
	14	778.55	2438.29	6080.38
270	2	1178.10	3253.77	6411.65
	6	1175.97	3224.94	6282.52
	10	1169.45	3136.30	5924.96
	14	1146.68	2844.24	5165.55
No crack		1178.33	3256.88	6425.88

Table 6. Strain energy of free-free beams with and without a crack†

Crack		1st mode		2nd mode		3rd mode	
Position (mm)	Depth (mm)	$\hat{U}_1(a)$	$U(0)$	$\hat{U}_2(a)$	$U(0)$	$\hat{U}_3(a)$	$U(0)$
30	2	873.515	873.172	483.681	482.754	232.309	231.276
	6	870.592	867.085	478.968	469.368	232.194	221.562
	10	861.522	848.287	463.980	427.243	235.144	197.871
	14	828.485	781.126	418.662	301.860	274.394	195.813
90	2	868.937	861.514	486.668	480.038	234.838	233.982
	6	826.413	757.120	511.649	457.004	252.997	246.991
	10	724.687	528.219	586.340	466.827	280.563	270.753
	14	558.370	225.118	727.348	602.922	305.402	296.887
150	2	871.825	856.712	484.176	484.160	234.093	231.936
	6	855.938	724.792	484.124	483.976	248.097	231.847
	10	825.797	491.692	483.837	482.959	275.240	245.538
	14	788.499	232.165	483.008	480.034	309.605	284.221
210	2	880.402	872.880	480.747	474.198	227.466	226.637
	6	935.264	857.303	446.543	398.851	193.310	188.721
	10	1056.550	770.114	352.274	280.470	145.954	140.851
	14	1222.880	493.017	203.704	168.856	108.135	105.120
270	2	874.641	874.298	485.613	484.683	232.399	231.366
	6	882.102	878.548	498.404	488.414	230.973	220.396
	10	904.762	890.863	532.389	490.236	209.857	176.592
	14	981.857	925.730	585.052	421.829	101.505	72.436

† $\hat{U}_i(a)$: strain energy of cracked structure vibrating at mode i ; $U_0(0)$: strain energy of uncracked structure. The units of strain energy are $\text{kg}-\text{m}^2/\text{s}^2$.

strain energies of the uncracked beam for different cases are listed in Table 6. The identified crack sizes and the errors in estimation are given in Table 7. Again, the errors are very small. Experimental investigation of cracked free-free beams was also performed to validate the present method (Lee, 1992). The results obtained experimentally are encouraging and the errors are less than 10%.

Table 7. Actual and identified crack sizes of free-free beam

Actual (target) crack		1st mode		Identified crack size 2nd mode		3rd mode	
Position (mm)	Depth (mm)	Depth (mm)	Error %	Depth (mm)	Error %	Depth (mm)	Error %
30	2	2.0168	0.8400	2.0158	0.7900	2.0170	0.8500
	6	6.0054	0.0900	6.0188	0.3133	6.0550	0.9167
	10	10.0075	0.0750	10.0640	0.6400	10.1737	1.7370
	14	14.0166	0.1186	14.1123	0.8021	14.2109	1.5064
90	2	2.0105	0.5250	2.0102	0.5100	2.0193	0.9650
	6	6.0096	0.1600	6.0116	0.1933	6.0145	0.2417
	10	10.0216	0.2160	10.0263	0.2630	10.0354	0.3540
	14	14.0194	0.1386	14.0417	0.2979	14.0655	0.4679
150	2	2.0097	0.4850	3.4003	70.0150	2.0103	0.5150
	6	6.0028	0.0467	6.1625	2.7083	6.0038	0.0633
	10	10.0014	0.0140	10.0419	0.4190	10.0145	0.1450
	14	14.0006	0.0043	14.0175	0.1250	14.0305	0.2179
210	2	2.0106	0.5300	2.0102	0.5100	2.0188	0.9400
	6	6.0096	0.1600	6.0115	0.1917	6.0144	0.2400
	10	10.0215	0.2150	10.0264	0.2640	10.0348	0.3480
	14	14.0194	0.1386	14.0418	0.2986	14.0653	0.4664
270	2	2.0200	1.0000	2.0111	0.5550	2.0160	0.8000
	6	6.0058	0.0967	6.0191	0.3183	6.0551	0.9183
	10	10.0074	0.0740	10.0639	0.6390	10.1738	1.7380
	14	14.0166	0.1186	14.1124	0.8029	14.2371	1.6936

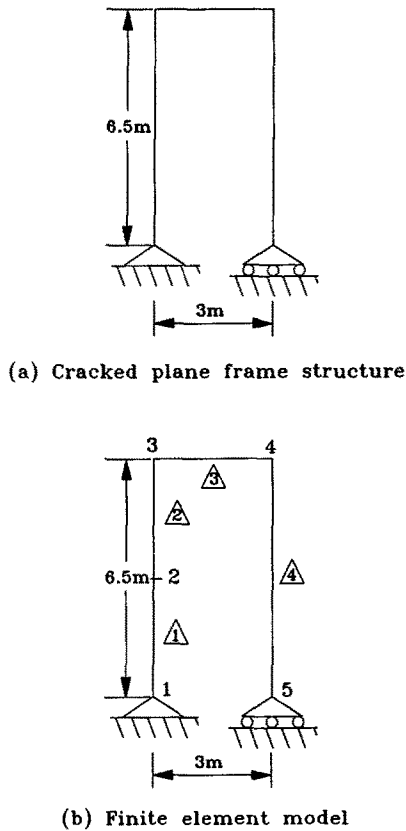


Fig. 8. Cracked plane frame and its finite element model for crack identification.

Finally, the present method was applied to crack size identification of the cracked frame in Fig. 8. The frame was composed of three beam members of cross-sectional dimensions, area = $14.0E-4 \text{ m}^2$, moment of inertia = $5.0E-6 \text{ m}^4$ and Young's modulus = $2.06E+11 \text{ kgf/m}^2$. The frame was discretized into four elements in the finite element model used for evaluating the frequencies and the mode shapes of the cracked frame. The crack was assumed to be located at the center of the cracked element of the frame. The frequencies of the frame containing cracks of different crack depth ratios (the ratio of crack size to the depth of member cross-section) are given in Table 8. The maximum modal strain energies of the cracked frame and the corresponding strain energies of the uncracked frame

Table 8. Natural frequencies of cracked plane frame structure

Crack		Natural frequency (Hz)		
Element no.	Depth ratio	1st	2nd	3rd
1	0.2	1.111	4.158	16.161
	0.4	1.107	4.152	15.831
	0.6	1.096	4.136	14.973
2	0.2	1.104	4.153	16.244
	0.4	1.073	4.131	16.229
	0.6	0.996	4.080	16.193
3	0.2	1.106	4.151	16.206
	0.4	1.084	4.121	16.051
	0.6	1.026	4.046	15.686
No crack		1.112	4.159	16.248

Table 9. Strain energy of plane frame structures with and without a crack†

Crack		1st mode		2nd mode		3rd mode	
Element no.	Depth (mm)	$\hat{U}_1(a)$	$U(0)$	$\hat{U}_2(a)$	$U(0)$	$\hat{U}_3(a)$	$U(0)$
1	41.4	2942.02	2936.66	2416.00	2414.29	85.556	84.635
	82.8	2946.19	2919.95	2403.51	2395.25	100.827	95.731
	124.2	2958.15	2870.96	2367.05	2340.56	144.758	123.320
2	41.4	2951.77	2908.42	2410.21	2403.25	81.590	81.548
	82.8	2991.12	2786.46	2377.45	2347.78	81.401	81.222
	124.2	3085.18	2471.04	2298.61	2230.14	80.995	80.565
3	41.4	2930.13	2899.52	2430.96	2421.38	79.167	78.755
	82.8	2889.89	2746.87	2474.68	2431.16	70.693	69.081
	124.2	2787.55	2369.13	2585.47	2467.92	53.550	50.535

† $\hat{U}_i(a)$: strain energy of cracked structure vibrating at mode i ; $U_0(0)$: strain energy of uncracked structure. The units of strain energy are $\text{kg} - \text{m}^2/\text{s}^2$.

for different cases are listed in Table 9. The identified crack sizes and the errors in estimation are given in Table 10. Again, the results show that the present method can yield very good results, even when only one vibration mode of the uncracked frame is used in the identification process.

7. CONCLUSIONS

A method for identifying the sizes of cracks on beam-type structures is presented. Concepts of modal analysis and fracture mechanics are used to construct an energy balance equation from which the size of the crack is evaluated via an iteration scheme. A few measured eigencouples of cracked and uncracked structures are required to compute the strain energies in constructing the energy balance equation. The present method is simple and easy to use and requires no information on the stiffness matrix of the structures. The use of the eigencouple of only one vibration mode of both cracked and uncracked structures can yield very good results so long as the crack is not located at the nodes of the mode. Examples of the identification of crack sizes for a fixed cantilever beam, a free-free beam and a plane frame are given to illustrate the applications and the accuracy of the present method. Factors that may affect the accuracy of identified crack size are also studied. Although the ideas and formulation presented in this paper are useful and valuable, the present method should be extended to the crack size identification of more complex structures before it can become a practical tool for nondestructive evaluation of damaged structures.

Table 10. Actual and identified crack sizes of plane frame structure

Actual (target) crack			Identified crack size					
Element no.	Depth ratio	Depth (mm)	1st mode		2nd mode		3rd mode	
			Depth (mm)	Error %	Depth (mm)	Error %	Depth (mm)	Error %
1	0.2	41.4	41.4007	0.0017	41.5114	0.2691	41.4068	0.0164
	0.4	82.8	82.7927	0.0088	82.8077	0.0093	82.8546	0.0659
	0.6	124.2	124.2033	0.0027	124.4580	0.2077	124.3279	0.1030
2	0.2	41.4	41.4018	0.0043	41.3917	0.0200	41.3774	0.0546
	0.4	82.8	83.0281	0.2755	82.8043	0.0052	82.8214	0.0258
	0.6	124.2	124.2052	0.0042	124.2030	0.0024	124.3281	0.1031
3	0.2	41.4	41.4038	0.0092	41.3934	0.0159	41.4143	0.0345
	0.4	82.8	82.8018	0.0022	82.7794	0.0249	82.8936	0.1130
	0.6	124.2	124.2084	0.0068	124.2155	0.0125	124.4966	0.2388

Acknowledgement—This research was supported in part by the National Science Council of the Republic of China through grant No. NSC 81-0401-E-009-10.

REFERENCES

- Anderson, T. L. (1991). *Fracture Mechanics—Fundamentals and Applications*. CRC Press, Boca Raton, FL.
- Anifantis, N., Aspragathos, N. and Dimarogonas, A. D. (1983). Diagnosis of cracks on concrete frames due to earthquakes by vibration response analysis. *Third Int. Symp. of the International Measurements Federation (IMEKO)*, Technical Committee on Technical Diagnostics, Moscow.
- Benjamin, J. R. and Cornell, C. A. (1970). *Probability, Statistics, and Decision for Civil Engineers*. McGraw-Hill, New York.
- Broek, D. (1974). *Elementary Engineering Fracture Mechanics*. Noordhoff, Leyden.
- Cawley, P. and Adams, R. D. (1979). Defect location in structures by a vibration technique. *American Society of Mechanical Engineers Design Engineering Technical Conf.*, St. Louis, Paper 79-DET-46.
- Chondros, T. G. and Dimarogonas, A. D. (1980). Identification of cracks in welded joints of complex structures. *J. Sound Vibr.* **69**(4), 531–538.
- Clough, R. W. and Penzien, J. (1975). *Dynamics of Structures*. McGraw-Hill, New York.
- Inagaki, T., Kanki, H. and Shiraki, K. (1981). Transverse vibrations of a general cracked rotor bearing system. *J. Mech. Des.* **104**, 1–11.
- Kam, T. Y. and Lee, T. Y. (1992). Detection of cracks in structures using modal test data. *Engng Fract. Mech.* **42**(2), 381–387.
- Lee, T. Y. (1992). Nondestructive evaluation of cracks in damaged structures using vibration data. Ph.D. dissertation, National Chiao Tung University, Hsin Chu, Taiwan.
- Lee, T. Y. and Kam, T. Y. (1993). A global minimization method for crack location identification. *J. Engng Optim.* **21**, 147–159.
- Qian, G. L. *et al.* (1990). The dynamic behaviour and crack detection of a beam with a crack. *J. Sound Vibr.* **138**(2), 233–243.
- Rizos, P. F. and Aspragathos, N. (1990). Identification of crack location and magnitude in a cantilever beam from the vibration modes. *J. Sound Vibr.* **138**(3), 381–388.
- Shen, M. H. H. (1989). Natural modes of cracked beams and identification of cracks. Ph.D. dissertation, University of Michigan, Ann Arbor.
- Tada, H., Paris, P. and Irwin, G. (1973). *The Stress Analysis of Cracks Handbook*. Del Research Corporation, Hellertown, PA.